

# Formation of Tetra(ethylene oxide) Terminated Si–C Linked Monolayers and Their Derivatization with Glycine: An Example of a Generic Strategy for the Immobilization of Biomolecules on Silicon

Till Böcking,<sup>†,‡</sup> Kristopher A. Kilian,<sup>‡</sup> Tracey Hanley,<sup>§</sup> Suhrawardi Ilyas,<sup>†</sup>  
Katharina Gaus,<sup>||</sup> Michael Gal,<sup>†</sup> and J. Justin Gooding<sup>\*,‡</sup>

School of Physics and School of Chemistry, University of New South Wales,  
Sydney, NSW 2052, Australia, Centre for Vascular Research, School of Medical Sciences,  
University of New South Wales, Sydney, NSW 2052, Australia, and The Bragg Institute,  
Australian Nuclear Science and Technology Organization (ANSTO), Lucas Heights Research  
Laboratory, Lucas Heights, NSW 2234, Australia

Received May 3, 2005. In Final Form: August 15, 2005

Surface modification with oligo(ethylene oxide) functionalized monolayers terminated with reactive headgroups constitutes a powerful strategy to provide specific coupling of biomolecules with simultaneous protection from nonspecific adsorption on surfaces for the preparation of biorecognition interfaces. To date, oligo(ethylene oxide) functionalized monolayer-forming molecules which can be activated for attachment of biomolecules but which can selectively form monolayers onto hydrogen terminated silicon have yet to be developed. Here, self-assembled monolayers (SAMs) containing tetra(ethylene oxide) moieties protected with *tert*-butyl dimethylsilyl groups were formed by thermal hydrosilylation of alkenes with single-crystal Si(111)–H. The protection group was used to avoid side reactions with the hydride terminated silicon surface. Monolayer formation was carried out using solutions of the alkene in the high-boiling-point solvent 1,3,5-triethylbenzene. The protecting group was removed under very mild acidic conditions to yield a free hydroxyl functionality, a convenient surface moiety for coupling of biological entities via carbamate bond formation. The chemical composition and structure of the monolayers before and after deprotection were characterized by X-ray photoelectron spectroscopy (XPS) and X-ray reflectometry. To demonstrate the utility of this surface for covalent modification, two reagents were compared and contrasted for their ability to activate the surface hydroxyl groups for coupling of free amines, carbonyl diimidazole (CDI), and disuccinimidyl carbonate (DSC). Analysis of XP spectra before and after activation by CDI or DSC, and after subsequent reaction with glycine, provided quantitative information on the extent of activation and overall coupling efficiencies. CDI activated surfaces gave poor coupling yields under various conditions, whereas DSC mediated activation followed by aminolysis at neutral pH was found to be an efficient method for the immobilization of amines on tetra(ethylene oxide) modified surfaces.

## Introduction

The rapid advances in biological discovery require the parallel progression of surface science to enable new biosensor and microarray technologies with greater sensitivity and reproducibility. Controlling the covalent immobilization of molecules on surfaces is key to developing strategies that allow the specific recognition of a biological species while reducing nonspecific interactions. Previously, a variety of methods for covalent immobilization of organic layers on surfaces have been utilized. Some common examples are alkylsilanes on glass and oxidized silicon,<sup>1,2</sup> alkanethiols on gold,<sup>1,3,4</sup> reaction of alcohols and aldehydes with hydride terminated silicon,<sup>5–7</sup> and alkene

and alkyne hydrosilylation with hydride terminated silicon.<sup>8,9</sup> Hydrosilylation of alkenes on hydride terminated silicon was first reported by Linford et al.<sup>10,11</sup> and has received much attention in the past decade leading to the development of a host of different wet chemistry techniques and experimental setups.<sup>8–10,12–25</sup> The formation of covalent Si–C bonds during hydrosilylation yields

\* To whom correspondence should be addressed. E-mail: Justin.Gooding@unsw.edu.au.

<sup>†</sup> School of Physics.

<sup>‡</sup> School of Chemistry.

<sup>§</sup> Bragg Institute.

<sup>||</sup> School of Medical Sciences.

(1) Dubrovsky, T. B. In *Protein Architecture*; Uri Lvov, H. M., Ed.; Marcel Dekker: New York, 2000; pp 25–54.

(2) Halliwell, C. M.; Cass, A. E. G. *Anal. Chem.* **2001**, *73*, 2476–2483.

(3) Gooding, J. J.; Mearns, F.; Yang, W.; Liu, J. *Electroanalysis* **2003**, *15*, 81–96.

(4) Witt, D.; Klajn, R.; Grzybowski, P. A. *Curr. Org. Chem.* **2004**, *8*, 1763–1797.

(5) Boukherroub, R.; Morin, S.; Sharpe, P.; Wayner, D. D. M.; Allongue, P. *Langmuir* **2000**, *16*, 7429–7434.

(6) Effenberger, F.; Götz, G.; Bidlingmaier, B.; Wezstein, M. *Angew. Chem., Int. Ed. Engl.* **1998**, *37*, 2462.

(7) Cleland, G.; Horrocks, B. R.; Houlton, A. *J. Chem. Soc., Faraday Trans.* **1995**, *91*, 4001.

(8) Buriak, J. M. *Chem. Rev.* **2002**, *102*, 1272–1306.

(9) Wayner, D. D. M.; Wolkow, R. A. *J. Chem. Soc., Perkin Trans. 2* **2002**, 23–34.

(10) Linford, M. R.; Chidsey, C. E. D. *J. Am. Chem. Soc.* **1993**, *115*, 12631–12632.

(11) Linford, M. R.; Fenter, P.; Eisenberger, P. M.; Chidsey, C. E. D. *J. Am. Chem. Soc.* **1995**, *117*, 3145–3155.

(12) Cicero, R. L.; Linford, M. R.; Chidsey, C. E. D. *Langmuir* **2000**, *16*, 5688–5695.

(13) Sieval, A. B.; Demirel, A. L.; Nissink, J. W. M.; Linford, M. R.; Maas, J. H. v. d.; Jeu, W. H. d.; Zuihof, H.; Sudhölter, E. J. R. *Langmuir* **1998**, *14*, 1759–1768.

(14) Wagner, P.; Nock, S.; Spudich, J. A.; Volkmut, W. D.; Chu, S.; Cicero, R. L.; Wade, C. P.; Linford, M. R.; Chidsey, C. E. D. *J. Struct. Biol.* **1997**, *119*, 189–201.

(15) Boukherroub, R.; Wayner, D. D. M. *J. Am. Chem. Soc.* **1999**, *121*, 11513–11515.

(16) Boukherroub, R.; Morin, S.; Bensebaa, F.; Wayner, D. D. M. *Langmuir* **1999**, *15*, 3831–3835.

(17) DiLabio, G. A.; Piva, P. G.; Kruse, P.; Wolkow, R. A. *J. Am. Chem. Soc.* **2004**, *126*, 16048–16050.

highly robust monolayers,<sup>26</sup> which are expected to be more stable than those prepared with thiols on gold or silanes on oxide surfaces. The high-density alkyl packing passivates the surface from oxidation, and atomically flat Si(111) can yield highly uniform self-assembled monolayers.<sup>14–16</sup>

We are particularly interested in exploiting the advantages of Si-C linked monolayers for developing biorecognition surfaces on flat and porous silicon for biosensing and cell capture applications. Achieving specific interaction between the surface and a sample analyte requires recognition molecules to interact with the species of interest while the remaining surface resists nonspecific adsorption of other sample components. With regard to the first feature, specific interaction with a species of interest, Si-C linked organic monolayer modified surfaces have shown considerable initial promise thus far, with recognition elements for DNA hybridization detection,<sup>27,29,30</sup> immobilization of saccharides,<sup>31</sup> peptides,<sup>32</sup> enzymes,<sup>33</sup> biomaterial applications,<sup>34</sup> drug delivery,<sup>35</sup> mass spectrometry,<sup>36</sup> metal-ion binding,<sup>37,38</sup> and other schemes developed for biomolecular conjugation.<sup>39–41</sup> Although these groups have made progress in the specific coupling of recognition elements, the second important criterion of the biorecognition interface, the ability to resist nonspecific adsorption of biomolecules, has received less attention. Self-assembled monolayers (SAMs) containing oligo(ethylene oxide) (OEO) moieties have been extensively

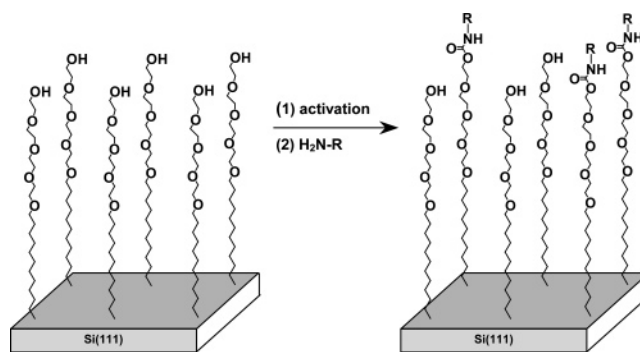


**Figure 1.** Strategy for the biomolecular modification of Si(111) using tetraethylene glycol terminated monolayers.

studied and have been shown to resist protein adsorption,<sup>42–46</sup> and recently, hydrosilylation of OEO containing alkenes on silicon has been reported.<sup>47–50</sup> A study by Yam et al.<sup>48</sup> characterized the antifouling properties of differing lengths of OEO molecules (EO<sub>n</sub>, *n* = 3, 6, and 9) on Si(111) by contact angle and X-ray photoelectron spectroscopy. Lasseter et al.<sup>50</sup> demonstrated the protein resistance of Si-C linked mixed monolayers formed from OEO and amine terminated alkenes by assaying the specific vs the nonspecific binding of common serum proteins and avidin on these surfaces. In an alternative approach, to impart inert properties onto Si-C linked monolayers, Voicu et al.<sup>29</sup> formed undecanoic acid terminated monolayers on Si(111) followed by coupling of amino terminated tetra-(ethylene oxide) derivatives.

As has been observed with alkanethiol chemistries, a powerful strategy for achieving both biorecognition and resistance to nonspecific adsorption is the fabrication of mixed self-assembled monolayers which incorporate OEO moieties in both the antifouling component and the molecule in which the biological molecule is coupled.<sup>51,52</sup> However, the design of an  $\omega$ -functionalized alkene for coupling is complicated by the potential of the terminal functionality (rather than the alkene) reacting with the Si-H surface. Although some groups have assumed these side reactions negligible,<sup>29,50</sup> eliminating competitive reactions between the  $\omega$ -functionality and the  $\alpha$ -alkene to obtain maximum uniformity of the monolayer (particularly with alcohols<sup>5</sup>) requires a protection strategy. The purpose of this paper is to report a new method of covalent modification and derivatization of the Si(111) surface with general applicability for the fabrication of biorecognition interfaces (Figure 1). Specifically, the thermal hydrosilylation of an  $\omega$ -protected EO<sub>4</sub> terminated alkene, (2-(2-(2-(2-(undec-10-enyloxy)ethoxy)ethoxy)-

(18) Lopinski, G. P.; Wayner, D. D. M.; Wolkow, R. A. *Nature* **2000**, *406*, 48–51.

(19) Takeuchi, N.; Kanai, Y.; Selloni, A. *J. Am. Chem. Soc.* **2004**, *126*, 15890–15896.

(20) Chazalviel, J.-N.; Vieillard, C.; Warntjes, M.; Ozanam, F. *Proc. Electrochem. Soc.* **1996**, *118*, 5375–5382.

(21) Buriak, J. M.; Allen, M. J. *J. Am. Chem. Soc.* **1998**, *120*, 1339–1340.

(22) Sieval, A. B.; Vleeming, V.; Zuilhof, H.; Sudhölter, E. J. R. *Langmuir* **1999**, *15*, 8288–8291.

(23) Linford, M. R.; Chidsey, C. E. D. *Langmuir* **2002**, *18*, 6217–6221.

(24) Niederhauser, T. L.; Lua, Y.-Y.; Sun, Y.; Jiang, G.; Strossman, G. S.; Pianetta, P.; Linford, M. R. *Chem. Mater.* **2002**, *14*, 27–29.

(25) Boukherroub, R.; Petit, A.; Loupy, A.; Chazalviel, J.-N.; Ozanam, F. *J. Phys. Chem. B* **2003**, *107*, 13459–13462.

(26) Sieval, A. B.; Linke, R.; Zuilhof, H.; Sudhölter, E. J. R. *Adv. Mater.* **2000**, *12*, 1457–1460.

(27) Strother, T.; Cai, W.; Zhao, X.; Hamers, R. J.; Smith, L. M. *J. Am. Chem. Soc.* **2000**, *122*, 1205–1209.

(28) Cha, T.-W.; Boiadjev, V.; Lozano, J.; Yang, H.; Zhu, X.-Y. *Anal. Biochem.* **2002**, *311*, 27–32.

(29) Voicu, R.; Boukherroub, R.; Bartzoka, V.; Ward, T.; Wojtyk, J. T. C.; Wayner, D. D. M. *Langmuir* **2004**, *20*, 11713–11720.

(30) Yin, H. B.; Brown, T.; Wilkinson, J. S.; Eason, R. W.; Melvin, T. *Nucleic Acids Res.* **2004**, *32*, e118.

(31) Smet, L. C. P. M. d.; Stork, G. A.; Hurenkamp, G. H. F.; Sun, Q.-Y.; Topal, H.; Vronen, P. J. E.; Sieval, A. B.; Wright, A.; Visser, G. M.; Zuilhof, H.; Sudhölter, E. J. R. *J. Am. Chem. Soc.* **2003**, *125*, 13916–13917.

(32) Coffinier, Y.; Olivier, C.; Perzyna, A.; Grandidier, B.; Wallart, X.; Durand, J.-O.; Melnyk, O.; Stiévenard, D. *Langmuir* **2005**, *21*, 1489–1496.

(33) Letant, S. E.; Hart, B. R.; Kane, S. R.; Hadi, M. Z.; Shields, S. J.; Reynolds, J. G. *Adv. Mater.* **2004**, *16*, 689–693.

(34) Canham, L. T.; Reeves, C. L.; Newey, J. P.; Houlton, M. R.; Cox, T. I.; Buriak, J. M.; Stewart, M. P. *Adv. Mater.* **1999**, *11*, 1505–1507.

(35) Anglin, E. J.; Schwartz, M. P.; Ng, V. P.; Perelman, L. A.; Sailor, M. J. *Langmuir* **2004**, *20*, 11264–11269.

(36) Meng, J.-C.; Averbuj, C.; Lewis, W. G.; Siuzdak, G.; Finn, M. G. *Angew. Chem., Int. Ed.* **2004**, *43*, 1255–1260.

(37) Ottenberg, C. M.; Crisp, F.; McDonald, J.; Evan, T.; O'Donnell, J.; Skrabal, S. A.; White, D. P. *Inorg. Chem.* **2002**, *41*, 7151–7158.

(38) Boiadjev, V. I.; Brown, G. M.; Pinnaduwa, L. A.; Goretzki, G.; Bonnesen, P. V.; Thundat, T. *Langmuir* **2005**, *21*, 1139–1142.

(39) Hart, B. R.; Letant, S. E.; Kane, S. R.; Hadi, M. Z.; Shields, S. J.; Reynolds, J. G. *Chem. Commun.* **2003**, *3*, 322–323.

(40) Bunimovich, Y. L.; Ge, G.; Beverly, K. C.; Ries, R. S.; Hood, L.; Heath, J. R. *Langmuir* **2004**, *20*, 10630–10638.

(41) Böcking, T.; James, M.; Coster, H. G. L.; Chilcott, T. C.; Barrow, K. D. *Langmuir* **2004**, *20*, 9227–9235.

(42) Prime, K. L.; Whitesides, G. M. *J. Am. Chem. Soc.* **1993**, *115*, 10714–10721.

(43) Harder, P.; Grunze, M.; Dahint, R.; Whitesides, G. M.; Laibinis, P. E. *J. Phys. Chem. B* **1998**, *102*, 426–436.

(44) Jiang, X.; Bruzewicz, D. A.; Thant, M. M.; Whitesides, G. M. *Anal. Chem.* **2004**, *76*, 6116–6121.

(45) Heuberger, M.; Drobek, T.; Vörös, J. *Langmuir* **2004**, *20*, 9445–9448.

(46) Vanderah, D. J.; La, H.; Naff, J.; Silin, V.; Rubinson, K. A. *J. Am. Chem. Soc.* **2004**, *126*, 13639–13641.

(47) Yam, C.-M.; Xiao, Z.; Gu, J.; Boutet, S.; Cai, C. *J. Am. Chem. Soc.* **2003**, *125*, 7498–7499.

(48) Yam, C. M.; Lopez-Romero, J. M.; Gu, J.; Cai, C. *Chem. Commun.* **2004**, *21*, 2510–2511.

(49) Gu, J.; Yam, C. M.; Li, S.; Cai, C. *J. Am. Chem. Soc.* **2004**, *126*, 8098–8099.

(50) Lasseter, T. L.; Clare, B. H.; Abbott, N. L.; Hamers, R. J. *J. Am. Chem. Soc.* **2004**, *126*, 10220–10221.

(51) Houseman, B. T.; Gawalt, E. S.; Mrksich, M. *Langmuir* **2003**, *19*, 1522–1531.

(52) Houseman, B. T.; Huh, J. H.; Kron, S. J.; Mrksich, M. *Nature Biotechnol.* **2002**, *20*, 270–274.

ethoxy)ethoxy)(*tert*-butyl)dimethylsilane (further referred to as C<sub>11</sub>-EO<sub>4</sub>-TBDMS), is reported. Surface reactions were carried out using dilutions of the alkene with 1,3,5-triethylbenzene as solvent to reduce the amount of alkene required for monolayer formation. Removal of the TBDMS group by deprotection yields a surface with terminal hydroxyl functionality, and subsequent derivatization is shown utilizing two common schemes for surface hydroxyl activation: carbonyl diimidazole and disuccinimidyl carbonate. Reaction of the model biological amine glycine with the activated surface demonstrates the utility for biomolecular conjugation. All surfaces and reaction steps are monitored and characterized by contact angle measurements, X-ray photoelectron spectroscopy, and X-ray reflectometry.

## Experimental Methods

**Materials.** All chemicals were reagent grade or higher and used as received unless stated otherwise. 1,3,5-Triethylbenzene (97%) was purchased from Fluka, redistilled from sodium under vacuum, and stored over molecular sieves under an argon atmosphere. Carbonyldiimidazole (CDI) was purchased from Aldrich, and *N,N'*-disuccinimidyl carbonate (DSC) was obtained from Fluka. Milli-Q water (18 M $\Omega$  cm) was used for rinsing samples and preparation of solutions. Ethanol, methanol, ethyl acetate, light petroleum, and dichloromethane were redistilled. Semiconductor-grade chemicals were used for cleaning (30% H<sub>2</sub>O<sub>2</sub>, 98% H<sub>2</sub>SO<sub>4</sub>) and etching (40% NH<sub>4</sub>F solution) pieces of a silicon wafer.

**Preparation of 2-(2-(2-(2-(Undec-10-enyloxy)ethoxy)ethoxy)ethoxy)ethoxy)ethanol (C<sub>11</sub>-EO<sub>4</sub>).** NaH (6.0 g, 250 mmol) was added to 100 mL of dry THF cooled on ice in a Schlenk flask. Tetraethylene glycol (52 mL, 390 mmol) was added in small portions to the stirred suspension. The reaction mixture was stirred on ice for 20 min followed by dropwise addition of 11-bromoundecene (10 mL, 95%, 43.3 mmol). The reaction was brought to room temperature and heated in an oil bath at 65 °C overnight. Water (2 mL) was added to remove any unreacted NaH, and the mixture was concentrated under reduced pressure followed by partitioning between ethyl acetate and brine. The aqueous phase was extracted twice with light petroleum, and the organic phases were combined, dried over Na<sub>2</sub>SO<sub>4</sub>, and concentrated under reduced pressure. The crude product was purified by column chromatography on silica (ethyl acetate/acetone 3:1 (v/v)) to yield C<sub>11</sub>-EO<sub>4</sub> as a colorless oil (11.04 g, 74%). <sup>1</sup>H NMR (300 MHz, CDCl<sub>3</sub>):  $\delta$  1.25 (12 H), 1.54 (quint, 2 H), 2.00 (m, 2 H), 2.78 (s, 1 H), 3.41 (t, 2 H), 3.52–3.64 (14 H), 3.69 (m, 2 H), 4.91 (m, 2 H), 5.77 (m, 1 H).

**Preparation of 2-(2-(2-(2-(Undec-10-enyloxy)ethoxy)ethoxy)ethoxy)ethoxy)(*tert*-butyl)dimethylsilane (C<sub>11</sub>-EO<sub>4</sub>-TBDMS).** *tert*-Butyldimethylsilyl chloride (1.36 g, 9.0 mmol) was added to a stirred solution of 2-(2-(2-(2-(undec-10-enyloxy)ethoxy)ethoxy)ethoxy)ethanol (2.6 g, 7.5 mmol) in dry CH<sub>2</sub>Cl<sub>2</sub> (8 mL) containing triethylamine (0.76 g, 7.5 mmol) and 4-(dimethylamino)pyridine (0.09 g, 0.75 mmol). The reaction mixture was stirred for 2 h, diluted with CH<sub>2</sub>Cl<sub>2</sub> (80 mL), and washed twice with water followed by a saturated aqueous ammonium chloride solution. The organic phase was dried over Na<sub>2</sub>SO<sub>4</sub> and concentrated under reduced pressure followed by vacuum with heating to yield C<sub>11</sub>-EO<sub>4</sub>-TBDMS as a colorless oil (3.32 g, 96%). For monolayer preparation, the compound was purified by vacuum distillation (5 mTorr, 162 °C) to give a colorless oil. The distilled product was stored over molecular sieves under an argon atmosphere. <sup>1</sup>H NMR (300 MHz, CDCl<sub>3</sub>):  $\delta$  0.05 (s, 6 H), 0.88 (s, 9 H), 1.27 (12 H), 1.56 (quint, 2 H), 2.01 (m, 2 H), 3.43 (t, 2 H), 3.52–3.57 (4 H), 3.61–3.65 (10 H), 3.75 (t, 2 H), 4.93 (m, 2 H), 5.79 (m, 1 H).

**Preparation of Si–C Linked Monolayers.** Si(111) wafers (*n*-type, 1–10  $\Omega$  cm, or *p*-type, 1–10  $\Omega$  cm) were cleaved into pieces (approximately 10  $\times$  15 mm<sup>2</sup>) and cleaned in concentrated H<sub>2</sub>SO<sub>4</sub>/30% H<sub>2</sub>O<sub>2</sub> (3:1, v/v) at 90 °C for 20–30 min followed by copious rinsing with Milli-Q water. **Caution!** Acidic solutions of concentrated hydrogen peroxides react violently with organic materials and should be handled with extreme care. Hydrogen

terminated Si(111) surfaces were prepared by etching in deoxygenated 40% solution of NH<sub>4</sub>F for 15–20 min. The 40% NH<sub>4</sub>F solution was deoxygenated by bubbling with argon for at least 30 min. Formation of monolayers by attachment of alkenes was achieved using thermal reaction in neat alkene or thermal reaction in a 0.2 M solution of the alkene in 1,3,5-triethylbenzene. The neat alkene or alkene solution was placed into a flame-dried Schlenk flask, degassed by five freeze–pump–thaw cycles, and placed under an argon atmosphere. After transfer of the freshly etched silicon wafer piece to the Schlenk flask, the flask was immersed in an oil bath at 200 °C for 2–6 h. Then the flask was opened to the atmosphere, and the sample was rinsed several times with dichloromethane and ethyl acetate and blown dry under a stream of argon.

**Derivatization of *tert*-Butyldimethylsilyl (TBDMS) Ether Terminated Surfaces.** (1) *Removal of the TBDMS Group.* Monolayers terminated with TBDMS ether groups were deprotected by immersion of the samples in a mixture of 32% HCl/95% ethanol (1:99, v/v) for 1 h to yield monolayers terminated by hydroxyl groups. The samples were then rinsed with ethanol and CH<sub>2</sub>Cl<sub>2</sub> and dried under argon.

(2) *Activation with Carbonyldiimidazole (CDI) and Reaction with Amines.* Silicon samples with hydroxyl terminated monolayers were immersed in a 0.25 M solution of CDI in anhydrous THF for 12 h under an argon atmosphere. The samples were rinsed with THF and CH<sub>2</sub>Cl<sub>2</sub> and blown dry under argon. Reaction with glycine was carried out using (a) 20 mM borate buffer with pH 8.5 containing 11 mM glycine for 24 h or (b) 100 mM carbonate buffer with pH 9.5 containing 33 mM glycine for 4 h. The samples were then rinsed with Milli-Q water, ethanol, and CH<sub>2</sub>Cl<sub>2</sub> and blown dry under argon.

(3) *Activation with *N,N'*-Disuccinimidyl Carbonate (DSC) and Reaction with Amines.* Silicon samples with hydroxyl terminated monolayers were immersed in a 0.1 M solution of DSC in dry DMF containing 0.1 M 4-(dimethylamino)pyridine for 3–12 h under an argon atmosphere. The samples were rinsed with DMF and CH<sub>2</sub>Cl<sub>2</sub> and blown dry under argon. Reaction with glycine was carried out using phosphate buffered saline containing 15 mM glycine for 4 h. The samples were then rinsed with Milli-Q water, ethanol, and CH<sub>2</sub>Cl<sub>2</sub> and blown dry under argon.

**XPS Measurements.** X-ray photoelectron (XP) spectra were obtained using an Escalab 220-IXL spectrometer with a monochromated Al K $\alpha$  source (1486.6 eV), a hemispherical analyzer, and a multichannel detector. The spectra were accumulated at a takeoff angle of 90° with a 0.79 mm<sup>2</sup> spot size at a pressure of less than 10<sup>-8</sup> mbar.

**Contact Angle Measurements.** Contact angles were determined using a Rame-Hart contact angle goniometer and the ImageJ software package for data analysis. Advancing and receding contact angles were measured with the needle embedded in the drop for addition and withdrawal of water, respectively. Static contact angles were determined by depositing a sessile drop onto the surface (needle withdrawn). The experimental error of the contact angle measurements is estimated to be  $\pm 2^\circ$ .

**X-ray Reflectometry.** X-ray reflectivity (XR) curves were measured on a Panalytical X'Pert Pro MPD with a Cu K $\alpha$  X-ray tube source configured for reflectometry. The configuration included an X-ray mirror for pseudoparallel beam optics, a beam size of 9 mm  $\times$  100  $\mu$ m, and a De-Wolf beam knife placed above the sample. The reflectivity data collected were analyzed using Parratt32 software.

## Results and Discussion

**Hydrosilylation of Alkenes with Si(111)–H in 1,3,5-Triethylbenzene.** Thermal hydrosilylation reactions for preparing Si–C linked monolayers are often carried out using neat alkenes,<sup>11,13,53</sup> which is convenient when the alkenes are inexpensive and commercially available or easy to prepare. However, for custom-synthesized alkenes, it is desirable to dilute these with suitable solvents to reduce the amount of alkenes required for surface de-

(53) Sieval, A. B.; Huisman, C. L.; Schönecker, A.; Schuurmans, F. M.; Van der Heide, A. S. H.; Goossens, A.; Sinke, W. C.; Zuilhof, H.; Sudhölter, E. J. R. *J. Phys. Chem. B* **2003**, *107*, 6846–6852.

**Table 1. Water Contact Angles in Degrees of Si(111) Derivatized with Organic Monolayers<sup>a</sup>**

	advancing	receding	static
Si-H + C <sub>18</sub> <sup>a</sup>			
C <sub>18</sub> , neat	110	104	109
C <sub>18</sub> , 0.2 M in 1,3,5-triethylbenzene	110	103	109
Si-H + C <sub>11</sub> EO <sub>4</sub> TBDMS <sup>b</sup>			
R-O-TBDMS (surface 1)	75	70	71
R-OH (surface 2)	47	40	45

<sup>a</sup> Formation of octadecyl monolayers using neat and diluted alkene. <sup>b</sup> TBDMS ether terminated monolayer before and after deprotection.

rivatization because of the cost and effort involved in their preparation. Sieval et al. have conducted a systematic study of various solvents and found that 1,3,5-trimethylbenzene (mesitylene, boiling point 162–164 °C) was the solvent of choice for the preparation of high-quality monolayers in dilute refluxing alkene solutions, possibly because the shape of the solvent molecule did not allow it to occupy holes in the monolayer and thus interfere with monolayer formation.<sup>22</sup> We have investigated thermal hydrosilylation reactions of alkenes in a 0.2 M solution in a similar solvent, 1,3,5-triethylbenzene. Because of its higher boiling point (215 °C), 1,3,5-triethylbenzene does not reflux at the temperature used for the hydrosilylation reaction (200 °C), thus allowing us to reduce the volume of the solution required for surface derivatization.

Monolayers prepared using neat and diluted octadecene were compared using XPS and water contact angles. XPS spectra of octadecyl derivatized Si(111) prepared in 1,3,5-triethylbenzene solutions of octadecene were similar to those prepared in the neat alkene. Both showed the expected carbon 1s peak along with the silicon 2s and 2p peaks, and a minor oxygen 1s peak was detectable.<sup>54</sup> The carbon content of a high-quality sample formed in diluted alkene was >90% of that found for the reference sample prepared in neat alkene. Water contact angles allow the assessment of the quality of methyl terminated alkyl monolayers because low coverage and disorder in the alkyl chains result in a significant decrease in the contact angle.<sup>55</sup> Octadecyl monolayers prepared from neat and dilute octadecene showed water contact angles that were indistinguishable within experimental error ( $\pm 2^\circ$ ), suggesting that both methods yielded layers of similar quality (Table 1). The advancing contact angle for both layers was 110°, consistent with that of ordered methyl terminated alkyl monolayers on Si(100)<sup>22</sup> and Si(111).<sup>11</sup>

The XPS and contact angle results demonstrated that high-quality alkyl monolayers could be formed when solutions of octadecene in 1,3,5-triethylbenzene are used. Therefore, this thermal method was used for the preparation of the functionalized monolayers described below.

**Chemistry of Monolayer Formation and Attachment of Amines.** Figure 2 shows the formation of tetra(ethylene oxide) terminated Si-C linked monolayers and the strategies investigated for covalent immobilization of amines on these monolayers. Reaction of hydride terminated silicon substrates with C<sub>11</sub>-EO<sub>4</sub>-TBDMS yielded TBDMS ether protected monolayers (surface 1). Removal of the TBDMS protecting group gave hydroxyl terminated

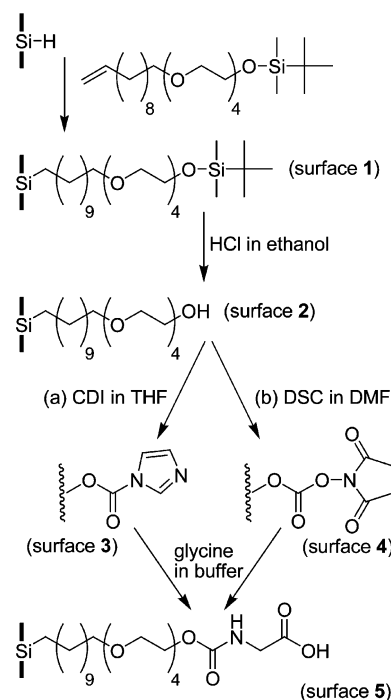


**Figure 2.** Strategies for the immobilization of amines on Si-C linked monolayers terminated with tetra(ethylene oxide) moieties.

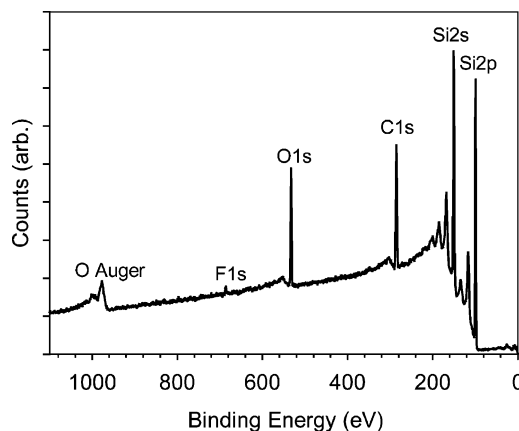


**Figure 3.** XP survey spectrum of a monolayer formed by thermal hydrosilylation of C<sub>11</sub>-EO<sub>4</sub>-TBDMS with Si-H.

monolayers (surface 2), which were activated using (a) CDI to give *N*-acylimidazole groups (surface 3) or (b) DSC to form succinimidyl carbonate groups (surface 4). Reaction of the activated surfaces 3 and 4 with glycine resulted in the coupling of glycine via carbamate linkages (surface 5).

**Preparation of C<sub>11</sub>-EO<sub>4</sub>-TBDMS Modified Silicon Surfaces.** Figure 3 shows the XP survey spectrum of a TBDMS ether protected monolayer (surface 1) prepared by thermal modification of hydride terminated Si(111) immersed in a 0.2 M solution of (2-(2-(2-(2-(undec-10-enyloxy)ethoxy)ethoxy)ethoxy)ethoxy)(*tert*-butyl)dimethylsilane (C<sub>11</sub>-EO<sub>4</sub>-TBDMS) in 1,3,5-triethylbenzene. The spectrum showed the silicon 2p and silicon 2s signals arising from the underlying substrate at ~99 and ~151 eV, respectively. The carbon and oxygen 1s peaks expected for the organic monolayer were seen at ~285 and ~533 eV, respectively. On a number of samples, a small peak at ~686 eV revealed the presence of low levels of fluoride ions on the silicon surface presumably from the etching step in ammonium fluoride solution.

(54) It was found that for both methods the quality of the monolayer as assessed by XPS (relative amounts of carbon, oxygen, and silicon) could vary among samples. Others have previously reported that the quality of Si-C linked monolayers is highly dependent on the care taken to avoid oxidation of the freshly etched Si-H surface<sup>14</sup> as well as the amount of oxygen and residual moisture present during the hydrosilylation reaction.<sup>12,53</sup>

(55) Folkers, J. P.; Gorman, C. B.; Laibinis, P. E.; Buchholz, S.; Whitesides, G. M.; Nuzzo, R. G. *Langmuir* **1995**, *11*, 813–824.

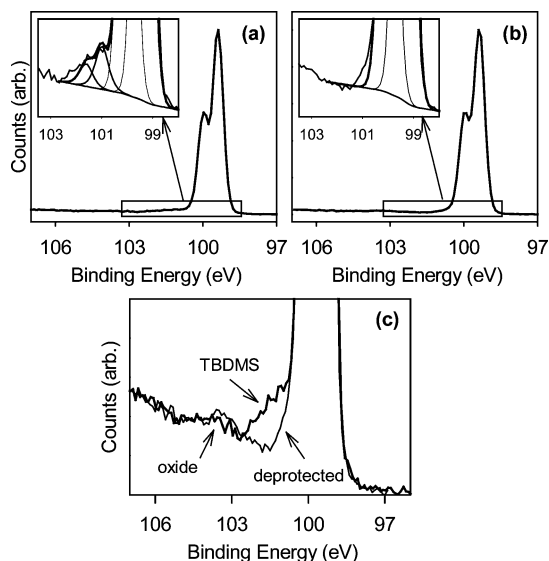


**Figure 4.** XP narrow scans of the silicon 2p region of the surface (a) terminated with TBDMS ether groups and (b) deprotected with 0.3% HCl in ethanol to yield hydroxyl groups. The expansions of both spectra are overlaid in panel c to show the presence and absence of the peak attributed to the silicon of the TBDMS groups before (thick line) and after (thin line) deprotection, respectively. The insets in panels a and b show the respective expansions with peak fits. The two components of each peak correspond to the silicon 2p<sub>1/2</sub> and 2p<sub>3/2</sub> components.

The carbon 1s, oxygen 1s, and silicon 2p narrow scans of surface **1** were consistent with a monolayer formed on the silicon substrate by reaction with C<sub>11</sub>-EO<sub>4</sub>-TBDMS. The silicon 2p region (Figure 4a) showed the peak arising from the bulk silicon with its 2p<sub>1/2</sub> and 2p<sub>3/2</sub> components at 100.0 and 99.4 eV, respectively. A slight shoulder was detectable on the high-binding energy side of the main silicon 2p peak (Figure 4a, inset). This shoulder disappeared after removal of the TBDMS protecting group under acidic conditions (vide infra) and was therefore attributed to the silicon of the TBDMS ether group of the organic monolayer. Peak fitting gave silicon 2p<sub>1/2</sub> and 2p<sub>3/2</sub> components at 101.6 and 101.0 eV, respectively. These values were similar to those observed for the silicon in the organic polymer poly(dimethylsiloxane) (102.4 and 101.8 eV).<sup>56</sup> The ratio of the silicon 2p peak area, attributed to the TBDMS group (Figure 4a), to the carbon 1s peak area was approximately 1:27, which was close to the ratio of 1:25 for the molecular structure of the C<sub>11</sub>-EO<sub>4</sub>-TBDMS molecule. The surface contained very low levels of silicon dioxide as the broad peak for oxidized silicon expected between 102 and 104 eV was only detectable in the expansion of the XP narrow scan (Figure 4c). The XP narrow scan of the oxygen 1s region (Figure 5) was dominated by the peak arising mainly from ether oxygens of the organic monolayer at 533.0 eV. A minor peak was seen at ~532 eV, which can be attributed to the bridging oxygen of the low levels of silicon dioxide<sup>57</sup> and/or the oxygen of the TBDMS ether. The carbon 1s envelope (Figure 6a) was fitted with two peaks. The peak at 285.0 eV was assigned to the carbons of the alkyl chain and those of the TBDMS group, whereas the peak at 286.8 eV was attributed to the C-O bonded carbons of the tetra-(ethylene oxide) moiety. The observed area ratio of the C-C/C-Si peak to the C-O peak was between 14.3:9 and

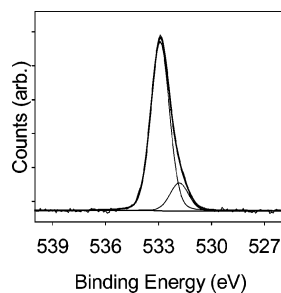


**Figure 5.** XP narrow scan of the oxygen 1s region of the surface terminated with TBDMS ether groups.

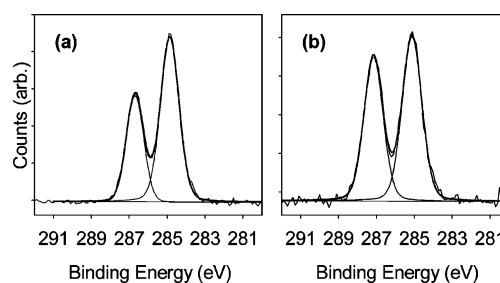


**Figure 6.** XP narrow scans of the carbon 1s region of the surface (a) terminated with TBDMS ether groups and (b) deprotected with 0.3% HCl in ethanol to yield hydroxyl groups.

15.9:9, which was consistent with the theoretical ratio of 16:9 for the monolayer composed of C<sub>11</sub>-EO<sub>4</sub>-TBDMS moieties.

**Removal of the TBDMS Protecting Group.** Conditions for the cleavage of the TBDMS ether were initially investigated in solution. In solution, the reaction of C<sub>11</sub>-EO<sub>4</sub>-TBDMS with 0.3% HCl in ethanol for 1 h gave nearly quantitative conversion (~99%) to the alcohol, as evidenced by thin-layer chromatography (TLC) and <sup>1</sup>H NMR spectroscopy. Removal of the TBDMS group under these conditions from surface **1** to yield a tetra(ethylene oxide) terminated monolayer (surface **2**) could be followed in the XP narrow scans of the silicon 2p (Figure 4b) and carbon 1s (Figure 6b) regions. The small signal of the TBDMS group at 101.0 eV present before deprotection was no longer detectable after treatment of the surface with dilute HCl in ethanol, which is clearly visible in the comparison of the respective silicon 2p narrow scans in Figure 4c. The carbon 1s region after deprotection (Figure 6b) showed a significant reduction in the signal at 285.0 eV relative to the signal at 287.0 eV due to the disappearance of the C-C and C-Si linked carbons of the TBDMS group. The peak area ratio for the C-C to the C-O binding energies was approximately 10.6:9, only marginally larger than the expected ratio of 10:9 for a completely deprotected monolayer. Deprotection under these conditions caused only minor degradation of the quality of the surface, as evidenced by a slight increase in the signal characteristic of silicon dioxide between 102 and 104 eV in the silicon 2p narrow scan (Figure 4c). The oxygen 1s region was also indicative of some increase in the oxide content.<sup>58</sup>

We used water contact angle measurements to confirm the cleavage of the TBDMS ether (Table 1). The advancing contact angles decreased from 75° for surface **1** to 47° for surface **2**. The latter was higher than the advancing water

(56) Beamson, G.; Briggs, D. *High-resolution XPS of organic polymers*; J. Wiley & Sons: New York, 1992.

(57) Uno, K.; Namiki, A.; Zaima, S.; Nakamura, T.; Ohtake, N. *Surf. Sci.* **1988**, *193*, 321–335.

(58) It was generally observed that the level of silicon dioxide associated with surface **1** varied among samples, and this was attributed to differences in the amount of moisture and oxygen present during the hydrosilylation reaction. Subsequent reactions led to a slight incremental increase in oxide associated with the surface after each reaction step, which has been observed for Si-C linked monolayers previously.<sup>27</sup>

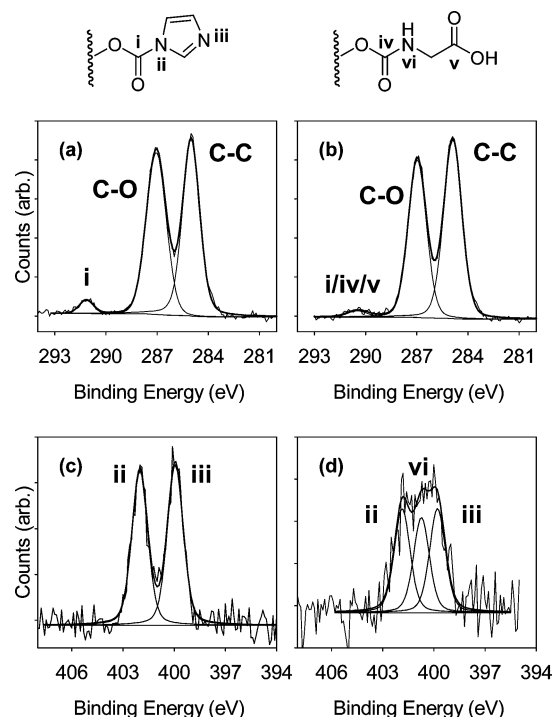


**Figure 7.** XP narrow scans of the carbon 1s (top panels) and the nitrogen 1s (bottom panels) regions of (a and c) the hydroxyl terminated surface after activation with CDI and (b and d) the activated surface after reaction with glycine.

contact angle of  $38^\circ$  for a similar self-assembled monolayer surface of tetra(ethylene oxide) terminated thiols on gold.<sup>59</sup>

#### Activation with CDI and Reaction with Amines.

The activation of the hydroxyl groups of surface **2** using CDI and the subsequent formation of carbamate linkages with glycine were investigated by XPS. The XP survey spectrum (not shown) of the CDI activated surface **3** showed the appearance of a nitrogen 1s signal at  $\sim 401$  eV in addition to the oxygen 1s, carbon 1s, and silicon 2s and 2p peaks at  $\sim 533$ ,  $\sim 286$ ,  $\sim 151$ , and  $\sim 99$  eV, respectively. Further evidence for the formation of *N*-acylimidazole groups on surface **3** came from the XP narrow scans of the carbon 1s, nitrogen 1s, and oxygen 1s regions. A new peak appeared at 291.1 eV in the carbon 1s spectrum (Figure 7a), consistent with the O-C(O)-N carbon of the *N*-acylimidazole intermediate. On the basis of the peak areas of the different carbon species, it was estimated that approximately 58% of the chains were activated. The nitrogen 1s region (Figure 7c) clearly showed the binding energies of the imine and amine nitrogens of the imidazole ring at 399.9 eV ( $=N-$ ) and 402.0 eV ( $-N<$ ), respectively, with the expected peak area ratio of 1:1.<sup>60,61</sup>

The reaction of the CDI activated surface **3** with glycine in an aqueous buffer at pH 8.5 did not go to completion even after allowing the reaction to proceed for 24 h. This was immediately evident from the XP narrow scan of the nitrogen 1s region (Figure 7d), which was deconvoluted into three components. The peaks at 399.9 and 402.0 eV, characteristic of the imidazole nitrogens, confirmed the presence of unreacted *N*-acylimidazole intermediates, whereas the peak at 400.8 eV indicated the formation of

**Table 2.** Terminal Group Composition in % of the CDI Activated Surface and after Reaction with Glycine

	surface 5		
	surface 3	pH 8.5, 24 h	pH 9.5, 4 h
R-OH (underivatized)	42	75	69
<i>N</i> -acylimidazole	58	12.5	26
R-O-C(O)-NH-CH <sub>2</sub> -COOH		12.5	5

carbamate linkages by reaction of the amino group of glycine with part of the activated chains. The carbon 1s spectrum (Figure 7b) of the surface showed a broad peak at 290.6 eV with a full width at half-maximum value of 1.4 eV. This peak was difficult to deconvolute but presumably contained contributions from the O-C(O)-N carbon from residual activated intermediates as well as those of the carbamate and carboxylic acid groups of the attached glycine. Table 2 shows the reaction yields for the activation and coupling steps based on the carbon 1s and nitrogen 1s peak areas of the respective surfaces. It was estimated that surface **5** prepared via CDI activation followed by reaction with glycine at pH 8.5 for 24 h consisted of  $\sim 75\%$  underivatized (hydroxyl terminated) chains and  $\sim 25\%$  derivatized chains; approximately half of those were present as the *N*-acylimidazole intermediate, and half were coupled to glycine. When we considered the relatively high level of activated chains on surface **3** ( $\sim 58\%$ ) and the reduced level of derivatized chains on surface **5**, it was apparent that more than half of the activated chains underwent hydrolysis back to a hydroxyl terminus. Long reaction times are undesirable for the preparation of biorecognition interfaces, and it is known that the reaction of *N*-acylimidazoles with amines proceeds more readily at an elevated pH. Consequently, we increased the pH in an attempt to increase the yield and reduce the reaction time. After coupling at pH 9.5 for 4 h, the reaction had also not gone to completion and the rate of hydrolysis was approximately 6 times faster than the rate of the coupling reaction, resulting in a low glycine surface coverage (Table 2). Because of the poor yields obtained with CDI mediated coupling, we investigated the use of DSC for the immobilization of glycine via carbamate linkages.

#### Activation with DSC and Reaction with Amines.

DSC is frequently used as a coupling agent to link alcohols and amines and has been employed for the derivatization of solid supports for DNA microchips<sup>62</sup> and the immobilization and patterning of proteins on Si(111).<sup>28,63</sup> Activation of the terminal hydroxyl groups with DSC to yield surface **4** was evident in the XP survey spectrum (not shown) by the appearance of a nitrogen 1s signal at  $\sim 401$  eV in addition to the previously detected elements. In the carbon 1s narrow scan (Figure 8a), two new peaks that shifted to higher binding energies were seen because of the introduction of the succinimidyl carbonate groups. The area ratio of the peak at 289.5 eV attributed to the two C=O carbons of the imide groups and the peak at 291.4 eV due to the O-C(O)-O carbon of the carbonate group was approximately 1.7:1, which was in reasonable agreement with expectation (2:1). The binding energy of the nitrogen of the NHS group was shifted to 402.6 eV (as shown in Figure 8c) similar to the shift observed for other NHS ester terminated monolayers.<sup>41</sup> The oxygen 1s envelope was difficult to deconvolute into its components because of a variety of binding energies for the organic

(59) Pale-Grosdemange, C.; Simon, E. S.; Prime, K. L.; Whitesides, G. M. *J. Am. Chem. Soc.* **1991**, *113*, 12–20.

(60) Vasnin, S.; Geanangel, R. A. *Inorg. Chim. Acta* **1989**, *160*, 167–170.

(61) Luo, X. F.; Goh, S. H.; Lee, S. Y.; Huan, C. H. A. *Macromol. Chem. Phys.* **1999**, *200*, 874–880.

(62) Beier, M.; Hoheisel, J. D. *Nucleic Acids Res.* **1999**, *27*, 1970–1977.

(63) Jun, Y.; Cha, T.; Guo, A.; Zhu, X. Y. *Biomaterials* **2004**, *25*, 3503–3509.

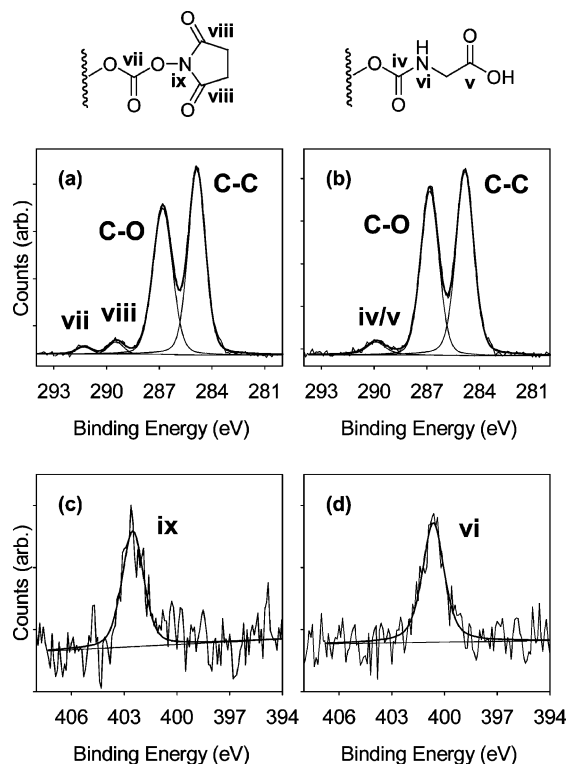


**Figure 8.** XP narrow scans of the carbon 1s region (top panels) and the nitrogen 1s region (bottom panels) of the hydroxyl terminated surface (a and c) after activation with DSC and (b and d) after reaction with glycine.

layer as well as an (unknown) contribution from low levels of oxidized silicon species. However, the main peak at 533.1 eV, which was previously attributed to the ether oxygens of the tetra(ethylene oxide) moieties, showed a pronounced shoulder at the high-binding energy side between 535 and 536 eV. The shoulder was assigned to the C–O–N linked oxygen of the NHS group, which is shifted to binding energies greater than 535 eV,<sup>29,41</sup> presumably with contributions also due to the  $\text{EO}_4\text{-O-C(O)}$  oxygen at an intermediate binding energy between the main ether oxygen and NHS oxygen peak. On the basis of the XPS data, it was estimated that ~45% of the chains on surface 4 were activated by DSC.

In contrast to the CDI mediated coupling on surface 3, the reaction of the DSC activated surface 4 with glycine proceeded smoothly at near neutral pH. The binding energies characteristic of the succinimidyl carbonate groups were no longer detectable in the carbon, nitrogen, and oxygen 1s spectra, indicating that the conversion had gone to completion. Instead, new binding energies were detected suggesting the immobilization of glycine on the monolayer via carbamate linkages. Notably, the nitrogen 1s binding energy of the carbamate occurred at 400.8 eV (as shown in Figure 8d) and shifted considerably toward lower binding energies compared to those of the nitrogen of the NHS group. The carbon 1s spectrum (Figure 8b) showed a signal at 290.1 eV in addition to the previously identified peaks at 285.0 and 287.0 eV. This peak was slightly broadened because of the slightly different binding energies from the C=O carbons of the carbamate and carboxylic acid groups of the attached glycine residues. The levels of activation on surface 4 and coupling on surface 5 are summarized in Table 3. The overall yield of chains in the monolayer with an attached glycine residue was ~38%, which was only slightly lower than the yield of activated chains in the previous step. Thus, the coupling

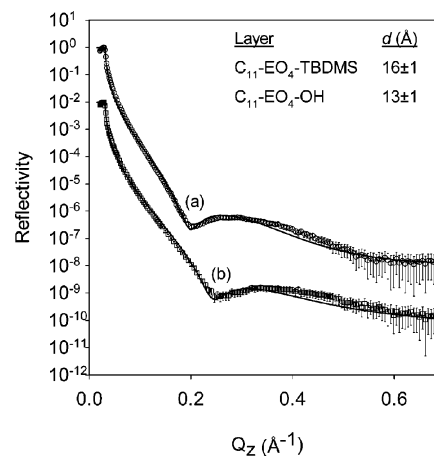


**Figure 9.** XR curves of (a) surface 1 and (b) surface 2. The solid lines represent model fits to the reflectivity data. Curve b has been offset for clarity.

**Table 3. Terminal Group Composition in % of the DSC Activated Surface and after Reaction with Glycine**

	surface 4	surface 5
R–OH (underivatized)	55	62
R–O–C(O)–O–NHS	45	0
R–O–C(O)–NH–CH <sub>2</sub> –COOH		38

reaction (~84%) was faster under the conditions used here than the competing hydrolysis reaction (~16%).

**X-ray Reflectometry.** Figure 9 shows the observed and fitted X-ray reflectivity (XR) curves as a function of momentum transfer ( $Q_z$ ) for the TBDMS protected surface 1 and the deprotected surface 2. Because of the ultrathin nature of the monolayers, only one minimum was observed before the background was reached. The shift of the minimum toward higher  $Q_z$  values after deprotection clearly indicated the reduction in the layer thickness, as expected for the removal of the TBDMS protecting group. The thickness and electron density of the organic films were determined by fitting a monolayer structural model to the observed data. The thickness of the TBDMS protected monolayer was determined on three independently prepared samples and was found to vary between 16 and 17 Å. This value was only about half of the calculated length of the fully stretched molecule (~32 Å). The smaller than expected thickness indicated that the layer was collapsed possibly as a result of a reduced grafting density.<sup>64,65</sup> After exposure to dilute HCl in ethanol, the thickness was reduced to 13–14 Å (determined on two independently prepared samples).<sup>66</sup> The decrease in thickness of ~3 Å was consistent with the removal of the TBDMS protecting group from the monolayer surface. Again, the thickness of the monolayer was considerably shorter than expected for the fully stretched molecule (~28 Å) and was also shorter than the ellipsometric thickness of 23 Å for a similar layer (terminated by tri(ethylene oxide) monomethyl ether) on Si(111).<sup>48</sup>

(64) Papra, A.; Gadegaard, N.; Larsen, N. B. *Langmuir* **2001**, *17*, 1457–1460.

(65) It has been reported that the chains of densely packed and well-ordered Si–C linked monolayers are uniformly tilted by ~30–45° from surface normal.<sup>11,13</sup> A tilting of the chains could also be considered here, but it appears unlikely that the chains are fully extended given the extent to which the layer thickness is reduced compared to the length of the molecule.

(66) We observed slight changes in the reflectivity curve for the same (deprotected) sample measured on different days, and these fluctuations were tentatively attributed to changes in the humidity and hence uptake of water into the ethylene oxide region of the monolayer.

The electron density could not be determined to a high degree of certainty with our system and varied between 0.4 and 0.5 e<sup>-</sup> Å<sup>-3</sup> for surface **1** and 0.4 and 0.6 e<sup>-</sup> Å<sup>-3</sup> for surface **2**. These values were higher than those for electron densities of Si-C linked alkyl monolayers (0.30–0.32 e<sup>-</sup> Å<sup>-3</sup>) on Si(111)<sup>11</sup> and Si(100),<sup>13</sup> as expected for the presence of ethylene oxide moieties, and were comparable to the value reported for self-assembled monolayers of low-molecular weight poly(ethylene oxide) silanes on silicon dioxide surfaces (0.44 e<sup>-</sup> Å<sup>-3</sup>).<sup>64</sup>

### Conclusions

Formation of Si-C linked monolayers on Si(111)-H by thermal hydrosilylation of alkenes in 1,3,5-triethylbenzene solutions gave high-quality organic monolayers similar to those prepared using neat alkenes, as judged by contact angles and XPS. This thermal method was applied to the formation of tetra(ethylene oxide) terminated Si-C linked monolayers on Si(111). Reaction of C<sub>11</sub>-EO<sub>4</sub>-TBDMS with Si(111)-H gave monolayers with little oxidation of the silicon surface. The TBDMS protecting group, required to avoid side reaction with the hydride terminated silicon surface, could subsequently be removed from the monolayer surface using mild conditions which did not degrade the quality of the surface. The thickness of the monolayer determined by XR was less than expected for the length of the molecule indicating collapse of the layer.

Coupling of the amino acid glycine to the hydroxyl terminated monolayer was investigated using two different coupling reagents, CDI and DSC. Although the activation with CDI was efficient, the subsequent coupling of amines to the *N*-acylimidazole groups on the monolayer surface was poor and accompanied by the competing hydrolysis reaction, especially at high pH. In contrast, the reaction of amines with DSC activated terminal hydroxyl groups proceeded smoothly at near neutral pH. With DSC as the activation reagent, coupling of amines to hydroxyl terminated monolayers proceeds faster and gives higher yields than CDI mediated coupling. Thus, the modification of a hydride terminated silicon surface with tetraethylene glycol terminated monolayers followed by activation with DSC is a generic strategy for the selective coupling of biomolecules to silicon surfaces which is applicable to the development of silicon-based platforms for biosensor or microarray applications.

**Acknowledgment.** This study was supported by the Australian Research Council and the Australian Institute for Nuclear Science and Engineering. The authors thank Dr. Michael James for help with the reflectivity measurements.

LA051191S